

## Stability of Hyperbolic Finite-Difference Models with One or Two Boundaries

Lloyd N. Trefethen<sup>1</sup>

**ABSTRACT.** The stability of finite-difference models of hyperbolic partial differential equations depends on how numerical waves propagate and reflect at boundaries. This paper presents an extended numerical example illustrating the key points of this theory.

**0. Introduction.** In the numerical solution of hyperbolic partial differential equations by finite differences, stability is well known to be a critical issue. As a first step, the difference model must satisfy the von Neumann condition—that is, the basic formula should admit no exponentially growing Fourier modes. For linear problems with smoothly varying coefficients and no boundaries, this is essentially the whole story, and in fact if one rules out algebraically as well as exponentially growing local Fourier modes, then stability is assured. Results of this kind are widely known and are discussed in the superb book by Richtmyer and Morton [8].

When boundaries are introduced, the stability problem becomes more subtle. Even here the literature is copious, and a dozen or more people have made substantial contributions, including Godunov and Ryabenkii, Strang, Osher [7], Kreiss, Gustafsson, Sundström, Tadmor, and Michelson. The best known paper in this area is the one by Gustafsson, Kreiss and Sundström [4] in 1972, which presents what is now often referred to

---

1980 *Mathematics Subject Classification.* Primary 65M10.

<sup>1</sup> Supported by an NSF Mathematical Sciences Postdoctoral Fellowship and by the U.S. Dept. of Energy under Contract DE-AC02-76-ER03077-V while the author was at the Courant Institute of Mathematical Sciences.

as the "GKS stability theory". The great strength of the GKS paper is that it establishes a necessary and sufficient stability condition for difference models of very general form—three-point or multipoint stencil in space, two-level or multilevel in time, explicit or implicit, dissipative or nondissipative. A difficulty with the paper is that it is very hard to read, and this has regrettably limited its influence. Fortunately, some more accessible accounts have appeared recently, including the report of Gustafsson in this volume.

My own work in this field has been concerned with giving the stability question for initial boundary value problem models a physical interpretation based on the ideas of dispersive wave propagation and group velocity. Group velocity effects in finite-difference modeling have been surveyed by me in [9] and by Vichnevetsky and Bowles in [13]; others who have been interested in these matters include Matsuno, Grotjahn and O'Brien in meteorology; Alfold, Bamberger, and Martineau-Nicoletis in geophysics; Kentzer, Giles and Thompkins in aerodynamics; and Hedstrom and Chin in theoretical numerical analysis. I have described a group velocity interpretation of the one-boundary stability problem in [10], showing in particular how the GKS "perturbation test" for unstable "generalized eigensolutions" is equivalent to a test of the sign of a group velocity. In [11] this approach is made rigorous, and various theorems on unstable growth rates are obtained. In [12] I have extended these ideas to problems with two or more boundaries or internal interfaces, where stability depends on what happens when wave packets reflect back and forth. The latter work was motivated in part by ideas of Kreiss (see, e.g., [4, §7]), of Beam, Warming and Yee [1], and of Giles and Thompkins [2].

There is an analogous theory for p.d.e.'s rather than difference approximations. Again, wave radiation from the boundary is a general mechanism of ill-posedness. See Kreiss [6] for the basic theory, and the new survey by Higdon [5] for the wave interpretation. The difference is that for p.d.e.'s, nontrivial cases of ill-posedness do not arise unless the domain contains two or more space dimensions.

The purpose of this paper is to survey these results relating stability and wave propagation by means of an extended example. With the aid of many illustrations we will see exactly how waves can get amplified by reflection at boundaries and how this can lead to instability.

**1. No boundaries: dispersive wave propagation.** As our basic difference scheme we will take the *Crank-Nicolson (CN)* or *trapezoidal* formula

$$v_j^{n+1} - v_j^n = \frac{\lambda}{4} (v_{j+1}^n + v_{j+1}^{n+1} - v_{j-1}^n - v_{j-1}^{n+1}) \quad (1.1)$$

for the p.d.e.  $u_t = u_x$ . Here  $j$  is the space index,  $n$  is the time index, and  $\lambda$  is the *mesh ratio*  $k/h$ , where  $k$  and  $h$  are the time and space steps, respectively. Because CN is a nondissipative, two-level formula, it will be easy to analyze how waves propagate. The price we pay for this is that CN is implicit, which means that in principle it cannot be implemented on an unbounded domain, although it still defines a bounded operator on  $l^2$ . However, this is no problem for simple test experiments, since we can keep the action away from the boundary when we wish.

A general initial data distribution  $v^0 \in l^2$  can be written as a Fourier integral

$$v_j^0 = \frac{1}{2\pi} \int_{-\pi/h}^{\pi/h} e^{i\xi x} \hat{v}^0(\xi) d\xi, \quad x = jh, \tag{1.2}$$

where the dual variable  $\xi$  is called the *wave number*. The Fourier transform  $\hat{v}^0$  is a  $2\pi/h$ -periodic function in  $L^2[-\pi/h, \pi/h]$  given by the Fourier series

$$\hat{v}^0(\xi) = \lim_{N \rightarrow \infty} \sum_{j=-N}^N e^{-i\xi x} v_j^0, \quad x = jh. \tag{1.3}$$

To determine what  $v^n$  will look like for  $n > 0$ , we can first determine what will happen to an initial sine wave  $e^{i\xi x}$  and then use Fourier synthesis. To this end, substitute  $e^{i(\omega t + \xi x)}$  in (1.1), where  $\omega$  is a *frequency* to be determined. The result is the equation

$$e^{i\omega k} - 1 = \frac{\lambda}{4} (e^{i\xi h} + e^{i(\omega k + \xi h)} - e^{-i\xi h} - e^{i(\omega k - \xi h)}),$$

which simplifies to

$$2 \tan \frac{\omega k}{2} = \lambda \sin \xi h. \tag{1.4}$$

This is the *numerical dispersion relation* for CN. This equation defines a unique value  $\omega \in [-\pi/k, \pi/k]$  for each  $\xi \in [-\pi/h, \pi/h]$ , and so it is actually a function

$$\omega(\xi) = \frac{2}{k} \tan^{-1} \left( \frac{\lambda}{2} \sin \xi h \right). \tag{1.4'}$$

Figure 1.1 shows what (1.4') looks like in the case  $\lambda = 1$ : For  $\xi h \ll \pi$  the dispersion function matches the ideal function  $\omega = \xi$  for  $u_t = u_x$  closely, but for larger  $\xi$  it disagrees markedly.

Now that the dispersion function is known we can synthesize  $v^n$  as follows:

$$v_j^n = \frac{1}{2\pi} \int_{-\pi/h}^{\pi/h} e^{i(\omega(\xi)t + \xi x)} \hat{v}^0(\xi) d\xi, \quad x = jh, t = nk. \tag{1.5}$$

Armed with this equation we could duplicate the behavior of CN by computing Fourier integrals. There is little profit in that, but what (1.5) does offer is the prospect of approximate evaluation by a stationary phase argument. For observe that the exponential term introduces an oscillatory behavior that will make the integrand tend to cancel to zero if  $\omega(\xi)$  and  $\delta^0(\xi)$  are smooth. The exception is that at values of  $\xi$  satisfying

$$\frac{d}{d\xi}(\omega(\xi)t + \xi x) = 0, \quad \text{i.e.} \quad \frac{d\omega(\xi)}{d\xi} = -\frac{x}{t},$$

there is no oscillation and no cancellation. In other words, most of the energy associated with wave number  $\xi$  travels approximately at the *group velocity*

$$C = -\frac{d\omega}{d\xi}. \quad (1.6)$$

Of course this argument is vague, but it can be made precise in various ways; see, for example, Lemma 5.1 of [11].

Thus wave energy travels at a velocity given by the negative of the slope of the dispersion relation. For CN we can differentiate (1.4) implicitly to obtain

$$C = -\cos \xi h \cos^2 \frac{\omega k}{2}. \quad (1.7)$$

Eliminating  $\omega$  by means of (1.4'), or differentiating (1.4') directly, converts this to the functional form

$$C(\xi) = \frac{-\cos \xi h}{1 + (\lambda^2/4) \sin^2 \xi h}. \quad (1.7')$$

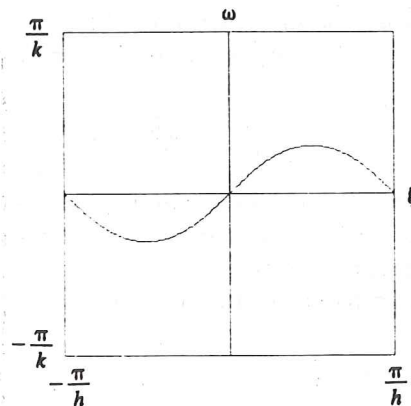


FIGURE 1.1. Dispersion relation for CN with  $\lambda = 1$ .

This function is plotted in Figure 1.2. One sees that for well-resolved waves—i.e.  $\xi h \ll 0$ , or many points per wavelength—energy travels at velocity  $-1$ , as it should according to the p.d.e.  $u_t = u_x$ . Less well-resolved waves have lower speeds (less negative velocities), and it is this fact that gives rise to familiar oscillations around discontinuities. At the extreme, the sawtoothed (or *parasitic*) wave  $v_j^n = (-1)^j$ , i.e.  $\xi h = \pm \pi$ , has group velocity  $+1$ , so energy in this mode travels in the physically wrong direction (Figure 1.2).

Let us confirm this last prediction by an experiment. Figure 1.3 shows the evolution under CN with  $h = .01$  and  $\lambda = 1$  of an initial signal

$$v_j^n = [1 + (-1)^j] e^{-400(x-.5)^2}$$

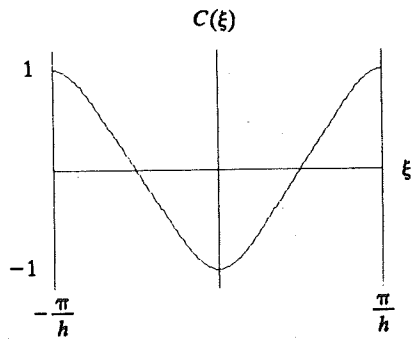


FIGURE 1.2. Group velocity.

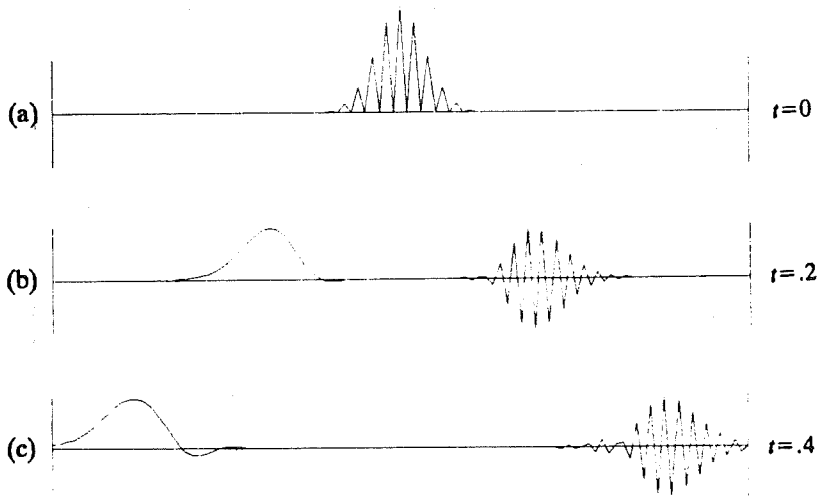


FIGURE 1.3. Propagation of energy at group velocities  $C = \pm 1$ .

on the interval  $[0, 1]$ . This “rectified Gaussian”, shown in Figure 1.3(a), contains equal amounts of energy at  $\xi h = 0$  and at  $\xi h = \pm\pi$ . Figures 1.3(b), (c) show the wave forms at times .2 and .4. As predicted, the two wave components have separated and traveled in opposite directions. This backwards motion of the parasitic wave component is of course a purely numerical effect. For further examples see [9 and 13].

In analyzing the behavior of an arbitrary difference model, a useful question to ask is: given a frequency  $\omega_0$ , what associated wave numbers  $\xi$  are admitted by the dispersion relation, and how do the corresponding waves  $\exp(i(\omega_0 t + \xi x))$  propagate? To get the answer for CN, imagine drawing a horizontal line at height  $\omega_0$  in Figure 1.1. Assuming  $\omega_0$  is small enough, it will intersect the dispersion curve at two values  $\xi_1$  and  $\xi_2$ . Of the two corresponding sine waves, one has  $C \leq 0$  and one has  $C \geq 0$ . For simplicity, from now on we will write  $\eta$  for the wave number corresponding to  $C \leq 0$  and  $\xi$  for the other one. By (1.4),  $\xi$  and  $\eta$  are related under CN by

$$\xi = \frac{\pi}{h} - \eta \quad \begin{array}{l} \xi: \text{rightgoing,} \\ \eta: \text{leftgoing.} \end{array} \quad (1.8)$$

The same relationship holds for any difference model, such as leap frog or backwards Euler, whose spatial discretization consists of the usual second-order centered difference.

As a more complicated example, suppose we had a nondissipative difference formula with the dispersion function plotted in Figure 1.4. (An arbitrary continuous dispersion function defines a bounded operator  $v^n \mapsto v^{n+1}$  in  $l^2$ , a *Fourier multiplier*, but this operator can be realized by finite differences only when the function is the solution of a trigonometric polynomial equation in  $\omega$  and  $\xi$ .) According to the figure, there are

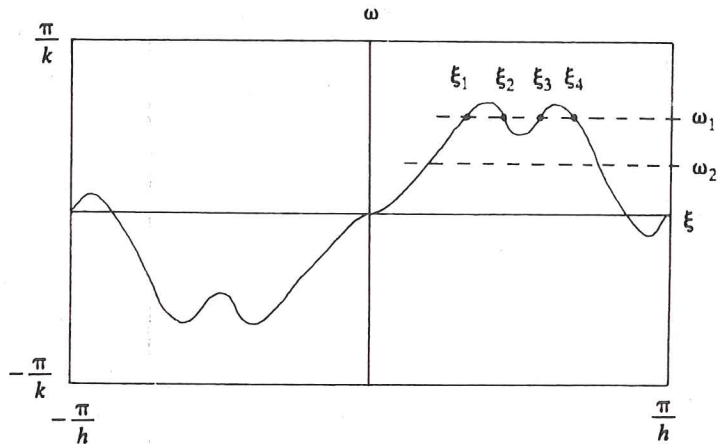


FIGURE 1.4. Dispersion relation for an unknown difference formula.

four wave numbers  $\xi_v$  associated with the frequency  $\omega_1$ .  $\xi_1$  and  $\xi_3$  correspond to leftgoing waves, and  $\xi_2$  and  $\xi_4$  to rightgoing waves.

On the face of it, the situation looks different at frequency  $\omega_2$ —there is only one wave propagating in each direction. However, in fact, the missing two wave numbers still exist, but they have become complex. One has negative imaginary part and corresponds to a leftgoing evanescent wave that does not carry energy; the other has positive imaginary part and is evanescent and rightgoing.

Actually, as far as one can tell from Figure 1.4, evanescent modes may exist at frequency  $\omega_1$  too. This depends on the size of the stencil of the difference formula. The general rule is this: for a scalar difference formula with stencil extending  $l$  points to the left of center and  $r$  points to the right, the dispersion relation is a trigonometric polynomial in  $\xi$  of degree  $l + r$ , which for each  $\omega$  has  $l + r$  complex roots  $\xi$  that break down into exactly  $r$  “leftgoing” and  $l$  “rightgoing” linearly independent wave modes. Here we say that a wave  $\exp(i(\omega t + \xi x))$  with  $\text{Im } \omega = 0$  (or more generally  $\text{Im } \omega \leq 0$ ) is *rightgoing* if either

- (1)  $\text{Im } \xi = 0$  and  $C(\xi, \omega) \geq 0$ , or
- (2)  $\text{Im } \xi > 0$ .

A *leftgoing* wave is defined with the directions of the inequalities in (1) and (2) reversed. These definitions and their consequences are studied in detail in [11].

Thus the general solution of the form  $v_j^n = e^{i\omega t} \phi_j$  to an arbitrary scalar finite-difference formula can be written

$$v_j^n = e^{i\omega t} \sum_{\substack{v=1 \\ \text{(rightgoing)}}}^l \alpha_v e^{i\xi_v x} + e^{i\omega t} \sum_{\substack{v=1 \\ \text{(leftgoing)}}}^r \beta_v e^{i\eta_v x}, \quad x = jh, t = nk. \tag{1.9}$$

For convenience I have relabeled  $\alpha_{l+1}, \dots, \alpha_{l+r}$  by  $\beta_1, \dots, \beta_r$ , and  $\xi_{l+1}, \dots, \xi_{l+r}$  by  $\eta_1, \dots, \eta_r$ .

**2. One boundary: reflection coefficients.** What if we now let more time elapse in Figure 1.3, so that the waves hit the boundaries at  $x = \pm 1$ ? The result will, of course, depend on the boundary conditions there.

The general principle for analyzing such problems is to look for solutions containing only a single frequency  $\omega_0$ . Different frequencies can be superposed later. If a wave  $\exp(i(\omega_0 t + \xi_0 x))$  hits a boundary, then the reflected result after the initial transient has died away will be a linear combination  $\sum \alpha_v \exp(i(\omega_0 t + \xi_v x))$  of waves with the same frequency  $\omega_0$  but with various new wave numbers  $\xi_v$ . In general, the wave numbers in the reflected waves will be all of those fulfilling the following two conditions:

- (1)  $\omega_0, \xi_v$  satisfy the dispersion relation.



(2) The wave  $\exp(i(\omega_0 t + \xi_v x))$  propagates away from the boundary into the interior (the *radiation condition*). This means that any wave reflected at a left-hand boundary must be rightgoing, and any wave reflected at a right-hand boundary must be leftgoing.

Neither of these statements mentions the boundary conditions. Those do not affect the set of reflected waves, just the coefficients  $\alpha_v$ .

To compute numerical reflection coefficients one simply inserts the wave (1.9) into the numerical boundary conditions. For a general formulation consider a left-hand boundary at  $x = j = 0$ , and let the numerical boundary conditions there consist of  $l$  linear homogeneous equations giving  $v_0^{n+1}, \dots, v_{l-1}^{n+1}$  as linear combinations of other values  $v_j^n$ . Insertion of (1.9) yields a linear *reflection equation*

$$E(\omega)\alpha = D(\omega)\beta, \quad (2.1)$$

relating leftgoing and rightgoing wave coefficients. Here  $E$  and  $D$  are matrices of dimensions  $l \times l$  and  $l \times r$ , respectively. If  $E(\omega)$  is nonsingular we can solve for the rightgoing wave coefficients to get

$$\alpha = A(\omega)\beta = [E(\omega)]^{-1}D(\omega)\beta. \quad (2.2)$$

$A(\omega)$  is called the *reflection matrix*. Compare [4, (10.2)].

Figure 2.1 shows what happens when the integration of Figure 1.3 is carried to  $t > 1/2$  with the following conditions at the boundaries:

$$v_0^{n+1} = v_1^{n+1}, \quad (2.3a)$$

$$v_j^{n+1} = 0. \quad (2.4a)$$

Here  $J = 1/h$  is the index of the grid point at the boundary  $x = 1$ . Figures 2.1(a), (b) show the configuration at times  $t = .6$  and  $t = .8$ . Clearly the leftgoing pulse with  $\eta = 0$  has generated a rightgoing reflected wave with  $\xi = \pi/h$  at very small amplitude. The rightgoing pulse with  $\xi = \pi/h$  has generated a considerably larger reflection with  $\eta = 0$ . Let us predict these reflected amplitudes after the fact.

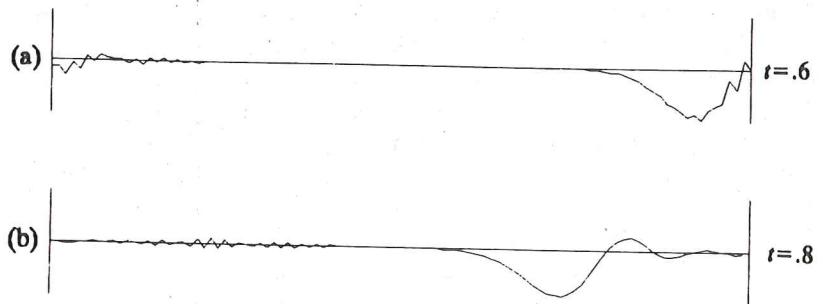


FIGURE 2.1. Continuation of Figure 1.3 showing reflection at boundaries.



First, we compute the reflection coefficient for (2.3a). In the present case, (1.8) implies that (1.9) reduces to

$$\begin{aligned} v_j^n &= [\alpha e^{i\xi x} + \beta e^{i\eta x}] e^{i\omega t} \\ &= [(-1)^J \alpha e^{-i\eta x} + \beta e^{i\eta x}] e^{i\omega t}, \quad x = jh, t = nk. \end{aligned} \quad (2.5)$$

For simplicity in such computations it is convenient to introduce the abbreviations

$$\kappa = e^{i\xi h}, \quad \mu = e^{i\eta h}, \quad z = e^{i\omega k}. \quad (2.6)$$

Then (2.5) becomes

$$v_j^n = (\alpha \kappa^j + \beta \mu^j) z^n. \quad (2.7)$$

For CN, (1.8) becomes  $\kappa = -1/\mu$ . Inserting (2.7) in (2.3a) gives

$$\alpha + \beta = (\alpha \kappa + \beta \mu) = -\alpha/\mu + \beta \mu.$$

In the form of (2.1) this is

$$\left(1 + \frac{1}{\mu}\right) \alpha = (\mu - 1) \beta, \quad (2.3b)$$

that is,

$$\frac{\alpha}{\beta} = \mu \frac{\mu - 1}{\mu + 1} = i e^{i\eta h} \tan \frac{\eta h}{2}. \quad (2.3c)$$

For  $\eta \approx 0$ , as in the present experiment, we get  $\alpha/\beta \approx 0$ , and this explains the very small amplitude of the pulse reflected from the left-hand boundary in Figure 2.1.

Now the analogous computation for (2.4a): Inserting (2.7) gives

$$\kappa^J \alpha = -\mu^J \beta, \quad (2.4b)$$

that is,

$$\frac{\alpha}{\beta} = -(-\mu^2)^J = (-1)^{J+1} e^{2i\eta}. \quad (2.4c)$$

Thus the amplitude of the reflected wave should be equal and opposite to that of the incident wave, regardless of  $\eta$ . Figure 2.1 confirms this nicely.

Let us return to the left-hand boundary and consider some alternative boundary conditions. Suppose we replace (2.3a) by

$$v_0^{n+1} = v_1^n. \quad (2.8a)$$

Then insertion of (2.7) leads to

$$\left(z + \frac{1}{\mu}\right) \alpha = (-z + \mu) \beta, \quad (2.8b)$$

or

$$\frac{\alpha}{\beta} = \mu \frac{\mu - z}{1 + \mu z} = \frac{ie^{i\eta h} \sin((\eta h - \omega k)/2)}{\cos((\eta h + \omega k)/2)}. \quad (2.8c)$$

Again this predicts a near-zero reflected amplitude for  $\eta \approx 0 \approx \omega$ . On the other hand, suppose we impose

$$v_0^{n+1} = v_2^{n+1}. \quad (2.9a)$$

The reflection equation is then

$$(1 - 1/\mu^2)\alpha = (\mu^2 - 1)\beta. \quad (2.9b)$$

This implies

$$\frac{\alpha}{\beta} = \mu^2 = e^{2i\eta h}, \quad (2.9c)$$

much as in (2.4c), at least for  $\eta \neq 0$ . At  $\eta = 0$ , (2.9b) has the form  $0\alpha = 0\beta$ , so it is not solvable except in a limiting sense.

Figure 2.2 plots results of experiments with boundary conditions (2.8a) and (2.9a). Figure 2.2(a) shows the initial condition, a leftgoing wave with  $\eta = 0$  on a mesh with  $h = .01$  for  $[0, 1]$ , and Figures 2.2(b), (c) show the results at  $t = 1$  under (2.8a) and (2.9a), respectively. The predicted reflection coefficients 0 and 1 are clearly in evidence. In fact, no reflected

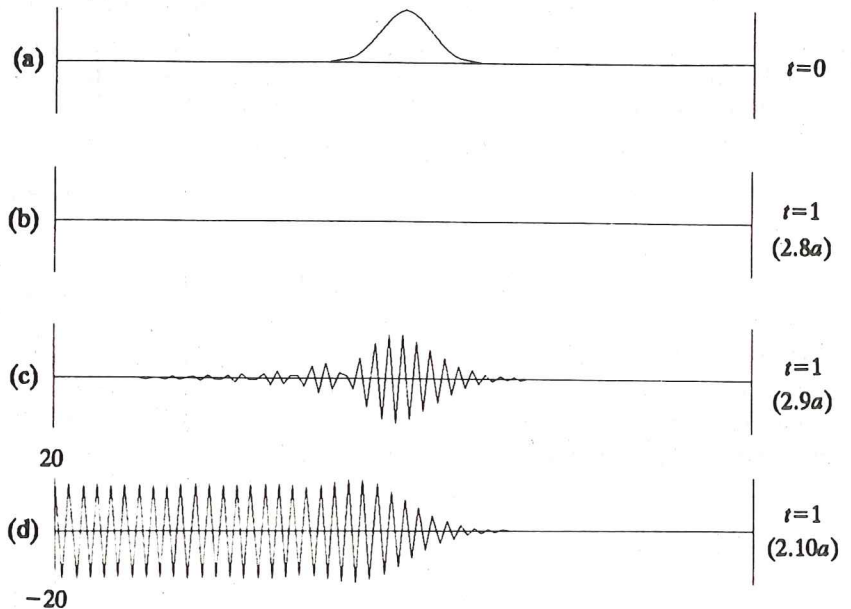


FIGURE 2.2. Effect of various left-hand boundary conditions.

energy at all is visible in Figure 2.2(b); this is because with  $\lambda = 1$ , i.e.  $h = k$ , (2.8c) is identically zero.

Figure 2.2(d) shows the response of CN to the same initial data with a more contrived boundary condition:

$$v_0^{n+1} = -v_1^{n+1} + v_2^{n+1} + v_3^{n+1}. \quad (2.10a)$$

This time a marked instability is evident (note the vertical scale). To see why, compute the reflection equation

$$[1 + \kappa - \kappa^2 - \kappa^3]\alpha = -[1 + \mu - \mu^2 - \mu^3]\beta,$$

which can be simplified to

$$(1 + \mu)(1 - \mu)^2\alpha = -\mu^3(1 + \mu)^2(1 - \mu)\beta, \quad (2.10b)$$

that is,

$$\frac{\alpha}{\beta} = -\mu^3 \frac{1 + \mu}{1 - \mu} = ie^{3i\eta h} \cot \frac{\eta h}{2}. \quad (2.10c)$$

At  $\eta = 0$ , this reflection coefficient is *infinite*.

The existence of a frequency  $\omega$  at which the reflection coefficient at a boundary is infinite implies that a finite-difference model is unstable. In [11] it is shown that under reasonable assumptions, such a model potentially amplifies initial data in the  $l^2$  norm at a rate at least proportional to the time step number  $n$ . Obviously this is an unstable situation, since as  $h$  and  $k$  are decreased, the index  $n$  corresponding to a fixed time  $\bar{t}$  increases to  $\infty$ .

The presence of an infinite reflection coefficient is a stronger condition than "GKS-instability," a name sometimes given to instability according to Definition 3.3 of [4]. In fact, a difference model is GKS-unstable if and only if the matrix  $E(\omega)$  in (2.1) is singular for some  $\omega$  with  $\text{Im } \omega \leq 0$ , i.e.  $|z| \geq 1$  (Theorem 1a of [11]). For scalar problems with three-point stencils, this amounts to the condition that the coefficient of  $\alpha$  on the left side of a reflection equation, such as (2.3b), (2.4b), (2.8b), (2.9b) or (2.10b), is 0 for some  $\omega$ . Thus, for example, the boundary condition (2.9a) is GKS-unstable for CN, since the left-hand side of (2.9b) is zero at  $\mu = z = 1$ , even though no apparent catastrophe occurred in Figure 2.2(c). In such situations the reflection coefficient remains finite if it happens that the right-hand side of the reflection equation has a zero at the same value of  $\omega$  of at least as high an order. When this occurs, it is shown in [11] that unstable growth of initial data in the  $l^2$  norm need proceed no faster than in proportion to  $\sqrt{n}$ .

To summarize, there are at least three distinct circumstances that may obtain at the boundary:

(1) nonsingular reflection equation, finite reflection coefficient: stable ( $\|v\| = O(1)$ );

(2) singular reflection equation, finite reflection coefficient: weakly unstable ( $\|v\| = O(\sqrt{n})$ );

(3) singular reflection equation, infinite reflection coefficient: unstable ( $\|v\| = O(n)$ ).

**3. Two boundaries: reflection back and forth.** What if we let even more time elapse in Figure 1.3 and 2.1? The answer is simple: new reflections will occur as the two wave packets bounce back and forth between  $x = 0$  and  $x = 1$ . Each time a rightgoing wave packet with  $\xi \approx \pi/h$  hits  $x = 1$ , it will reflect as a leftgoing wave packet with  $\eta \approx 0$  having essentially the same amplitude. But each time a leftgoing wave hits  $x = 0$ , it will reflect as a rightgoing wave of greatly diminished amplitude. The total energy in  $[0, 1]$  will consequently decay rapidly to near 0. The reason one can only say "near" is that a certain portion of the energy will have  $\xi \approx \pi/2h$ , and since  $C = 0$  at this wave number, this portion tends to stay in a fixed position and never hit the boundaries.

Figures 3.1(a), (b) confirm this prediction by showing the numerical solutions at  $t = 2$  and  $t = 4$ . At  $t = 2$  the signal that remains is very weak, and at  $t = 4$  it is somewhat weaker.

Suppose, more generally, that we set up the CN model on an interval  $[0, L]$  with some pair of stable boundary conditions at  $x = 0$  and  $x = L$  for which the reflection coefficient functions are  $A_1(\omega)$  and  $A_2(\omega)$ , respectively. If  $v^0$  is a wave packet with frequency  $\omega$ , then as  $t$  increases this packet will reflect back and forth, undergoing amplification by  $|A_1|$  or  $|A_2|$  each time it hits a boundary. Let  $C(\omega)$  denote the group speed  $|C(\xi, \omega)| = |C(\eta, \omega)|$ . Then the travel time for a complete circuit involving a reflection at each boundary will be

$$T(\omega) = \frac{2L}{C(\omega)}. \quad (3.1)$$

After such a circuit the amplitude will have increased by a factor

$$\alpha(\omega) = |A_1(\omega)A_2(\omega)|. \quad (3.2)$$

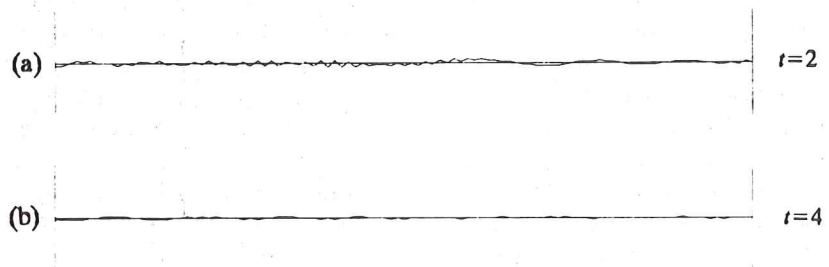


FIGURE 3.1. Further continuation of Figures 1.3 and 2.1.

Combining these formulas, we reach the following conclusion: as  $t \rightarrow \infty$ , energy associated with frequency  $\omega$  grows approximately at the rate

$$\frac{\|v(t)\|}{\|v(0)\|} \approx \alpha(\omega)^{t/T(\omega)} = \alpha(\omega)^{tC(\omega)/2L}. \quad (3.3)$$

For  $\alpha > 1$  this equation predicts exponential growth, and for  $\alpha < 1$ , exponential decay.

On the basis of this analysis one can now make some very interesting observations about stability and convergence. The following ideas are spelled out in detail in [12].

The first observation is: *stability does not preclude exponential growth in time*. We have seen in the last section that stability for a single boundary implies  $|A| < \infty$ , but not  $|A| \leq 1$ . Thus it is easily possible for a model composed of two individually stable boundaries to generate growth of truncation errors at a rate  $\exp(\text{const } t)$ . One might think that this reveals that the concatenation of two stable boundaries is in general unstable. But in fact, exponential growth does not imply instability in the usual Lax-Richtmyer sense, and it will not prevent convergence. The reason is that the growth factor for any fixed  $t$  does not get larger as  $h, k \rightarrow 0$ , whereas the truncation errors that the factor multiplies get smaller (by consistency).

These conclusions are already known. In fact, Theorem 5.4 of [4] asserts that in general, the concatenation of two GKS-stable difference schemes is always GKS-stable, while §7 of [4] investigates the conditions under which exponential growth in  $t$  will occur for a particular stable  $2 \times 2$  example. What is new here is the interpretation by reflection coefficients. This interpretation also helps to clear up a misconception. Some people have thought that although exponential growth can occur for finite  $h$  and  $k$ , it must vanish as  $h, k \rightarrow 0$ . But the study of reflecting wave packets gives no reason to expect such good fortune, and an example in [12] proves that, indeed, it is not to be expected. To be sure of eliminating growth by refining the mesh, one needs a difference formula that is suitably dissipative [3, 12].

There is a reason why exponential growth in  $t$  may be a problem: in practice, time-dependent finite-difference models are often used (especially in aerodynamics) to compute approximate solutions for the steady state  $t \rightarrow \infty$ . Obviously growth of errors at a rate  $e^{\text{const } t}$  will make such a procedure fail. With this in mind, Beam, Warming and Yee [1] have defined a difference model to be *P-stable* if it is GKS-stable and, in addition, it admits no exponentially growing modes. In this language the above observation becomes: stability does not imply *P-stability*.

Our second observation now comes as the natural complement to the first: *having reflection coefficients bounded by 1 does preclude exponential*

*growth in time.* For in (3.3) we see that if  $\alpha(\omega) \leq 1$  for every  $\omega$ , then no frequency exists that can experience repeated amplification by reflection. This argument can be made rigorous, and Proposition 10 of [12] states: if  $\alpha(\omega) \leq 1$  for every  $\omega$ , a difference model is *P*-stable.

For a third and final observation, let us turn to the case in which one or both boundaries is individually unstable. Then we find: *a mildly unstable boundary with an infinite reflection coefficient may become catastrophically unstable when a second boundary is introduced.* For consider a boundary condition which has  $A(\omega_0) = \infty$  for some  $\omega_0$ . If a wave packet at frequency  $\omega_0$  hits this boundary, it will be amplified by a large factor (typically  $O(N)$ , where  $N$  is the width of the packet in grid points). For a single boundary, this is a one-time-only event, as in Figure 2.2(d). But when there are two boundaries, the reflected wave may reflect at the other boundary, then return to be amplified again, and so on. For boundaries separated by  $N$  grid points one gets growth potentially at a very rapid rate

$$\frac{\|v(t)\|}{\|v(0)\|} \approx N^{\text{const } t} = N^{\text{const } nk}.$$

This instability is a far cry from the growth proportional to  $n$  mentioned in the last section, and it renders the difference model totally useless.

This phenomenon of catastrophic two-boundary interactions was first noted long ago by Kreiss. The advantage of the present point of view is that it makes it clear that the problem is associated not with all unstable boundaries, but only with those having infinite reflection coefficients. Unstable boundary conditions with finite reflection coefficients typically exhibit only weak instability even when other boundaries are present. Of course, sometimes weak instabilities may be more dangerous than strong ones, since they can more easily go undetected.

Our final numerical experiment, summarized in Figure 3.2, illustrates the difference in two-boundary behavior between unstable boundary conditions with finite and infinite reflection coefficients. Figure 3.2(a) shows the initial data, a uniformly distributed random signal on the usual CN mesh on  $[0, 1]$ . At  $x = 1$  the boundary condition is (2.4a). First, an integration was performed with the boundary condition (2.9a) at  $x = 0$ , which is unstable but by (2.9c) has a finite reflection coefficient. In this process nothing dramatic occurs no matter how large  $t$  is. Figures 3.2(b) show the result at  $t = 10$ , and it looks qualitatively much like the initial data. Of course this does not imply that this model will give accurate answers to physical problems, but it does reveal that GKS-instability of a boundary condition does not by itself lead to explosive two-boundary interactions.

In contrast, Figures 3.2(c), (d) show results obtained with boundary condition (2.10a), which has an infinite reflection coefficient. The plots show times  $t = 1, 3$ . Note the vertical scales.

In summary, for two-boundary problems one has the following possibilities:

- (1) stable b.c.'s,  $0 \leq \alpha \leq 1$ : stable and  $P$ -stable ( $\|v\| = O(1)$ );
- (2) stable b.c.'s,  $1 < \alpha < \infty$ : stable but  $P$ -unstable ( $\|v\| = O(e^{\text{const } t})$ );
- (3) unstable b.c.'s,  $0 \leq \alpha < \infty$ : weakly unstable ( $\|v\| = O(\sqrt{n})$ );
- (4) unstable b.c.'s,  $\alpha = \infty$ : strongly unstable ( $\|v\| = O(N^{\text{const } t})$ ).

Before closing, a word must be said about dissipation. I have presented a picture in which numerical waves bounce back and forth between boundaries, with changes of amplitude occurring at each reflection but not during the transit in between. Under a dissipative difference formula, however, any wave with  $\xi \neq 0$  decays as it travels. The result is that the two-boundary interactions I have spoken of rarely take place, so that in practice, the behavior of a dissipative two-boundary model is not much different from what the individual boundaries would suggest. The exceptions occur when the dissipation is very weak, as in the problems with large mesh ratios considered in [1], or when the number of grid points between boundaries is very small, as in certain cases discussed in §2 of [12].

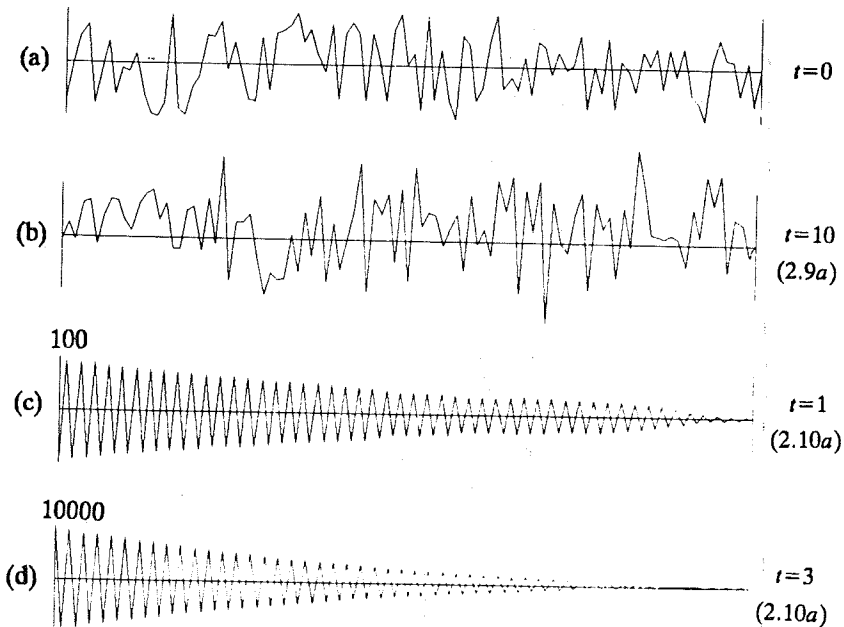


FIGURE 3.2. Two-boundary interactions.



For an overall summary, one may say that difference models for hyperbolic partial differential equations exhibit three important physical processes: propagation, reflection, and dissipation of waves. In general, the waves involved are numerical objects with no physical meaning, but they are still important to stability. An exact mathematical analysis of a finite-difference model is usually too difficult to be practical, but even for complicated models one can often gain insight fairly easily by considering these physical processes.

#### REFERENCES

1. R. M. Beam, R. F. Warming and H. C. Yee, *Stability analysis for numerical boundary conditions and implicit difference approximations of hyperbolic equations*, Proc. NASA Sympos. on Numerical Boundary Condition Procedures (Moffett Field, CA, October 1981), NASA, 1982, pp. 199–207.
2. M. Giles and W. Thompkins, Jr., *Asymptotic analysis of numerical wave propagation in finite difference equations*, Gas Turbine and Plasma Phys. Lab. Report 171, Mass. Inst. Tech., 1983.
3. B. Gustafsson, *The choice of numerical boundary conditions for hyperbolic systems*, Proc. NASA Sympos. on Numerical Boundary Condition Procedures (Moffett Field, CA, October 1981), NASA, 1982, pp. 209–225.
4. B. Gustafsson, H.-O. Kreiss and A. Sundström, *Stability theory of difference approximations for initial boundary value problems. II*, Math. Comp. **26** (1972), 649–686.
5. R. Higdon, *Initial-boundary value problems for linear hyperbolic systems*, Tech. Summer Report 2558, Math. Res. Cent., University of Wisconsin, Madison, 1983.
6. H.-O. Kreiss, *Initial boundary value problems for hyperbolic systems*, Comm. Pure Appl. Math. **23** (1970), 277–298.
7. S. Osher, *Systems of difference equations with general homogeneous boundary conditions*, Trans. Amer. Math. Soc. **137** (1969), 177–201.
8. R. D. Richtmyer and K. W. Morton, *Difference methods for initial-value problems*, Interscience, New York, 1967.
9. L. N. Trefethen, *Group velocity in finite difference schemes*, SIAM Rev. **24** (1982), 113–136.
10. ———, *Group velocity interpretation of the stability theory of Gustafsson, Kreiss, and Sundström*, J. Comput. Phys. **49** (1983), 199–217.
11. ———, *Instability of difference models for hyperbolic initial boundary value problems*, Comm. Pure Appl. Math. **37** (1984), 329–367.
12. ———, *Stability of finite difference models containing two boundaries or interfaces*, Math. Comp., submitted.
13. R. Vichnevetsky and J. B. Bowles, *Fourier analysis of numerical approximations of hyperbolic equations*, SIAM, Philadelphia, Pa., 1982.

DEPARTMENT OF MATHEMATICS, COURANT INSTITUTE OF MATHEMATICAL SCIENCES, NEW YORK UNIVERSITY, NEW YORK, NEW YORK 10012

*Current address.* Massachusetts Institute of Technology, Cambridge, Massachusetts 02139